CONF-9208146--1

DE92 040887

Invited paper for

Proceedings of the International Conference on
Computer Simulations of Radiation Effects in Solids,
Hahn-Meitner Institute Berlin
Berlin, Germany

August 23–28 1992

THE BINARY COLLISION APPROXIMATION: BACKGROUND AND INTRODUCTION

Mark T. Robinson

SOLID STATE DIVISION
OAK RIDGE NATIONAL LABORATORY
Managed by
MARTIN MARIETTA ENERGY SYSTEMS, INC.
Under
Contract No. DE-AC05-84OR21400
With the
U. S. DEPARTMENT OF ENERGY
OAK RIDGE, TENNESSEE

August 1992

THE BINARY COLLISION APPROXIMATION: BACKGROUND AND INTRODUCTION

Mark T. Robinson
Solid State Division, Oak Ridge National Laboratory,
Oak Ridge, Tennessee 37831-6032, U. S. A.

ABSTRACT

The binary collision approximation (BCA) has long been used in computer simulations of the interactions of energetic atoms with solid targets, as well as being the basis of most analytical theory in this area. While mainly a high-energy approximation, the BCA retains qualitative significance at low energies and, with proper formulation, gives useful quantitative information as well. Moreover, computer simulations based on the BCA can achieve good statistics in many situations where those based on full classical dynamical models require the most advanced computer hardware or are even impracticable.

The foundations of the BCA in classical scattering are reviewed, including methods of evaluating the scattering integrals, interaction potentials, and electron excitation effects. The explicit evaluation of time at significant points on particle trajectories is discussed, as are scheduling algorithms for ordering the collisions in a developing cascade. An approximate treatment of nearly simultaneous collisions is outlined and the searching algorithms used in MARLOWE are presented.

1. INTRODUCTION

The possibility of using digital computers to simulate the behavior of assemblies of atoms occurred independently to several groups in the late 1950s [1-6]. The earliest calculations used greatly simplified potentials or were even two-dimensional, but from these modest beginnings has come the whole field of the computer simulation of the interactions of energetic atoms with solids. Most of the work cited was supported by the old United States Atomic Energy Commission and, indeed, much of it was inspired by the many new research results then being obtained on the effects of neutron irradiation on the properties of matter, by the needs of the emerging nuclear fission power technologies, or by the more speculative ones of fusion power development. Partly as a result of computational efforts in this field, energetic ions became widely used as probes of condensed matter and as means of altering the composition, geometry, and properties of solids. These uses, in turn, inspired more elaborate computer models. Enormous advances in computing machinery and in software development have facilitated such developments. The hardware-limited calculations of 35 years ago, using programs written in assembly language or even in native numerical machine language, have been replaced by programs written in FORTRAN or C, executing at least 1000 times faster on relatively inexpensive workstations. And the end is not yet: massively parallel computers now promise further advances just as great over the next few years.

From the beginning, two different approaches were taken to the simulation of radiation effects in solids (for reviews, see [7-10]). One of these, the molecular dynamics (MD) method, proposed to integrate the equations of motion of numerical crystallites of a few hundred atoms until an initial disturbance was dissipated. The MD method, first used in radiation effects studies by Gibson, Goland, Milgram, and Vineyard [4], was originally constrained by computer limitations to the simulation of small numbers of individual events at initial kinetic energies below ~0.5 keV. Hardware developments have greatly relaxed

such constraints: MD codes can now follow collision cascades involving 10^4 to 10^5 atoms for simulated times of a few picoseconds. Nevertheless, there will long be computations too massive for widespread study by MD, where swifter, but more approximate, computational methods are needed. Such applications include achieving precise statistics, where large numbers of cascades must be evaluated; cascade studies in complex materials, such as noncubic compounds, where it is difficult to determine potentials reliably; cascade studies at high energies; and the like. Methods for such computations are the subject of this paper.

The binary collision approximation (BCA) has a long history in analytical theories of the slowing down of energetic atoms in matter [11], besides its uses in the kinetic theory of gases and other areas of statistical physics [12,13]. It seems to have been first used for an atomic collision calculation by Bredov et al. [2], who studied the penetration of 4 keV K^+ ions in Ge, probably using a hard-core approximation to Bohr's exponentially screened Coulomb potential. It was used by Goldman, Harrison, and Coveyou [3] to study the sputtering of a structureless copper target by 30 – 300 keV D^+ ions. Each incident ion was allowed to produce only one target knock-on. The target atoms interacted according to hard-core scattering with an average mean free path between collisions. At about the same time, Beeler and Besco [5,14,15] began their studies of collision cascades, originally using 5 keV ^{127}I slowing down in a two-dimensional model of BeO. It may be of interest that this work was a part of research supporting development of a nuclear-powered aircraft. Beeler and Besco used an impact-parameter-dependent hard-core approximation. For discussions of this and other so-called matching potential methods, see [16-19].

Also at about this time, work began in Oak Ridge that originally aimed at testing an analytical theory of particle ranges developed by Holmes and Leibfried [20]. Our original work [6,21,22] used a structureless target, but a model based on a crystalline target was soon developed [23,24] and this made possible the prediction of ion channeling. In both codes, Gaussian quadrature methods were used to evaluate the classical scattering integrals

using realistic (though still simplified) interaction potentials. These investigations seem to be the first in which the BCA was employed with an accurate representation of the scattering. However, since the codes only followed the primary particles and did not generate cascades, no attention was given to the temporal aspects of slowing down, which were neglected until recently.

Two classes of BCA models must be distinguished. In one of these, typified by MARLOWE [25], the locations of potential target atoms are determined by a well-defined crystal structure. Sigmund et al. [26] describe such models as BC programs. Aleatory (stochastic) methods play at most an auxiliary role in such codes, supplying, for example, initial primary particle positions or directions, local disorder, either thermal or chemical, and the like. Because of the regular structure, there are several important kinds of correlations among collisions in these models, of which channeling and linear collision sequences (LCSs) are the most familiar.

Targets in the other class of BCA models are structureless. In these Monte Carlo (MC) codes, aleatory methods are used to locate potential target atoms or to determine impact parameters, flight distances, scattering angles, and so on. There are no correlations between target sites, except those imposed by the density of the substance. Unlike MD and BC codes, the number of atoms in an MC code is not usually conserved, since there are no definite sites to identify the origins of atoms. The best known MC models are the family of TRIM codes [27].

There is confusion in the literature between the BC and MC classes of model, originating in part from the unfortunate practice of some authors of referring to MARLOWE as a "Monte Carlo" code, which it is not. This term should be confined to codes like TRIM [27] and ACAT [28], which use aleatory techniques in a fundamental way. BC codes are in several respects closer in spirit to MD codes than they are to MC codes. See, for example, the results of a recent round-robin collaboration on sputtering simulations [26].

The next section of this paper describes the BCA in some detail as it is implemented in the current version of MARLOWE [29,30]. This is followed by discussions of methods for evaluating the classical scattering integrals, of suitable potential energy functions for BCA calculations, and of inelastic energy loss functions. Much of this material is appropriate to both BC and MC codes, although the emphasis is on the former. A brief description is then given of a method of treating nearly simultaneous collisions in BCA models, an essential feature in obtaining realistic low-energy behavior in BC codes. The discussion then turns to algorithms for scheduling the collisions in BCA codes and for managing tables of particles, both important in developing efficient BC programs. Finally, a brief comparison of BC and MD models is presented.

2. THE BINARY COLLISION APPROXIMATION

The principal assumption of the binary collision approximation is that the interactions of energetic projectiles may be separated into a series of distinct two-body encounters. Such separation requires that changes in the relative energy of the interacting atoms be confined to the immediate vicinity of the target atoms, so that deflection of the projectiles is completed on a scale smaller than interatomic distances in the crystal. The situation is illustrated in Fig. 1. A projectile of mass m_1 and initial kinetic energy E_0 is located at a point P_0 at a time taken as the origin of a local time coordinate. A target atom of mass m_2 is initially at rest at the point T_0, the origin of the local space coordinates. The mass ratio $A = m_2/m_1$. The points P_0 and T_0 are separated by a distance L, sufficiently large that interactions between the two particles may be ignored. Figure 1 defines the impact parameter p, the barycentric scattering angle θ, the time integral τ, and the laboratory scattering angles ϑ and ϕ; the particles and the barycenter are shown at the apsis in the collision. The barycenter continues moving to the right until the scattered particles reach the points P_f and T_f, also separated by the distance L beyond which interactions are ignored.

The properties of the projectiles are evaluated at points such as P_a, T_a. Properties at intermediate points are not specified, but may often be found by interpolation. The calculation is formulated so that particles appear to move at constant speed along straight line segments, but their accelerations are, in fact, fully accounted for, as the following development will show. For example, the kinetic energy and time assigned to a projectile as it leaves P_a are already corrected for changes in speed that occur along the outgoing leg of the trajectory. These evaluations are exact, within the framework of isolated two-body encounters and numerical quadratures that are employed.

The model uses a quasielastic approximation in which a local inelastic (electron excitation) energy loss Q occurs at the apsis in an encounter, a loss taken from the kinetic energy of the barycenter. The time for the second part of the encounter is increased by a factor 1/f, where

$$f = [1 - (1+A)\, Q/A\, E_0]^{1/2} \tag{1}$$

The laboratory scattering angles are related to the barycentric angles by

$$\begin{aligned} \tan \vartheta &= A\, f \sin\theta / (1 + A\, f \cos\theta) \\ \tan \phi &= f \sin\theta / (1 - f \cos\theta) \ . \end{aligned} \tag{2}$$

The laboratory asymptotes to the particle trajectories intersect in the points P_a, T_a, found by evaluating the magnitudes x_1, x_2 (see Fig. 1):

$$\begin{aligned} x_1 &= [(1 + f)\, \tau + (f\, A - 1)\, p \tan(\theta/2)] / f\, (1 + A) \\ x_2 &= p \tan(\theta/2) - x_1 \end{aligned} \tag{3}$$

The latter is the length of the incoming asymptote to the target trajectory. The length of the incoming asymptote to the projectile trajectory is $\hat{\zeta} = \zeta - x_1$, where $\zeta = (L^2 - p^2)^{1/2}$. The kinetic energies of the two particles after scattering are

$$\begin{aligned} E_1 &= [(1 - f\, A)^2 + 4\, f\, A \cos^2(\theta/2)]\, E_0 / (1 + A)^2 \\ E_2 &= [(1 - f)^2\, A + 4\, f\, A \sin^2(\theta/2)]\, E_0 / (1 + A)^2 \end{aligned} \tag{4}$$

If the target atom must surmount a binding energy E_b to escape from its lattice site, its kinetic energy is reduced to $E_2 - E_b$. MARLOWE can employ different values of E_b for collisions in which the target is displaced, for those in which it is replaced by the projectile, and for those in which the target is a stopped cascade atom or an initial nonlattice atom.

As the two particles move from P_0, T_0 to the apsis, the barycenter moves a distance $(\zeta - \tau)/(1 + A)$ at a speed $v_0 / (1 + A)$; $v_0 = (2E_0/m_1)^{1/2}$ is the initial speed of the projectile. The time taken is $(\zeta - \tau)/v_0$. The time for the second part of the event is increased by the factor 1/f, because of the local inelastic energy loss. The calculation of the coordinates of P_a, T_a accounts for changes in the speed of the particles as they approach the apsis; to allow for changes as they leave it, the time t_a is assigned to both particles at the apsis, where

$$v_0 t_a = \zeta^* = \zeta + (1/f)[p \tan(\theta/2) - (1 + f)\tau] \quad . \tag{5}$$

As they leave the apsis, the particles are regarded as moving with the constant speeds $(2 E_1/m_1)^{1/2}$ and $(2 E_2/m_2)^{1/2}$, respectively. Finally, when a nonlocal energy loss is included in the model, the time t_a is increased by a factor $-(1/q)\ln(1 - q)$, where $q = nkE_0^{-1/2} \zeta^{1/2}$, n is the target density, and $k E_0^{1/2}$ is the nonlocal inelastic stopping cross section. Binding of the target atom to its site is ignored in evaluating t_a.

Equations (1-5) constitute the BCA for the case where the target atom is initially at rest. They may be generalized to the case where both particles are initially in motion. Yamamura [31] discusses some aspects of this case; further discussion is found in standard works on classical mechanics [32,33].

Comments are in order on the differences between the BCA as described here and the treatments of elastic scattering found in standard texts. The latter discuss the case where the scattered particles are detected in an apparatus at a macroscopic laboratory distance from the site of the collision. On this scale, the distances in Fig. 1 are negligible and the collision can be regarded as occurring at the initial target location. Only one scattering integral, the barycentric scattering angle, is needed. Here, however, the role of the detector

is taken by the next collision partners of the scattered particles, which are distant by amounts typical of the interatomic distances in crystals. In this situation, a second scattering integral, the so-called time integral, must be evaluated in order to locate the particle trajectories correctly in space and time. In addition, these remarks show the nature of approximations inherent in the BCA. When any of the lengths p, x_1, x_2, or the collision apsis is comparable to interatomic distances, separation of trajectories into distinct collisions is difficult. At low energies, large impact parameters are required to obtain an adequate representation of the nuclear (elastic) stopping cross section and the other quantities, especially x_1 and the apsis, can become large also.

In addition, the standard discussions ignore the temporal aspects of scattering, which are also insignificant on the laboratory scale. Collision times may be important in accurate simulations, however. The evaluation of apsidal times, t_a in Eq. (5), permits the proper time ordering of the events in a BCA calculation, thus removing one important difference with MD modelling. This topic will be addressed further below. In addition, knowledge of the time allows realistic modelling of several collision-based phenomena. As an example, see the study of Auger electron emission by Overbury et al. [34].

3. THE CLASSICAL SCATTERING INTEGRALS

The classical equations of motion may be solved in barycentric coordinates to yield the barycentric scattering angle [32,33]:

$$\theta = \pi - 2\,p \int_R^\infty dr\,[r^2\,g(r)]^{-1} = \pi - p\,I_1 \qquad (6)$$

and the time integral [19,24,25]:

$$\tau = (R^2 - p^2)^{1/2} - I_2 \qquad (7)$$

where

$$I_2 = \int_R^\infty dr\{[g(r)]^{-1} - (1 - p^2/R^2)^{-1/2}\}, \tag{8}$$

$$g(r) = [1 - p^2/r^2 - v(r)]^{1/2}, \tag{9}$$

$$v(r) = (1 + A)\, V(r) / A\, E_0, \tag{10}$$

r is the interatomic separation, V(r) is the interatomic potential energy, and R is the apsis in the collision, defined by g(R) = 0. Discussions of classical scattering (and some simulation models) also use the differential scattering cross section

$$d\sigma = (4 \pi p / \sin \theta)\, (d\theta / dp)^{-1}. \tag{11}$$

It is convenient to replace $d\theta/dp$ by an integral representation [35]:

$$d\theta/dp = (1/K - 1)\, I_1 + (1/K)\, I_3 \tag{12}$$

where

$$K = 1 - R^3\, v'(R) / 2\, p^2 \tag{13}$$

$$I_3 = \int_R^\infty (dr/r)\, [r\, g(r)]^{-3}\, [R^3\, v'(R) - r^3\, v'(r)]\ . \tag{14}$$

It is assumed in writing the integrals that L is large enough to be taken as infinite. This simplifies evaluation of the integrals and is consistent with the general picture of binary encounters. Since g(R) = 0, the integrands are singular at the lower limits, but they are integrable as long as $p^2 K > 0$, or $v'(R) < 2 p^2 / R^3$, a condition met by any potential with a repulsive core. The integral I_2 also requires $\lim_{r\to\infty} r\, v(r) = 0$, which is obeyed by all plausible potentials except the Coulomb potential.

There are several methods of evaluating the scattering integrals accurately. The singularities may be removed by substituting $r = R/(1 - u^2)$; the explicit forms for I_1 and I_2 are given in [36]. The transformed integrals can be evaluated by Gauss-Legendre quadrature [37] as was done in the early Oak Ridge simulation codes [21,24]. However, a

more efficient method is Gauss-Mehler quadrature [37], first used in classical scattering by F. J. Smith [38-40]. The substitution is r = R/u. The integrals become

$$I_1 = (2/R) \int_0^1 du(1 - u^2)^{-1/2} [(1 - u^2)^{1/2} / G(u)]$$
$$I_2 = R \int_0^1 du(1 - u^2)^{-1/2} [(1 - u^2)^{1/2}\{G(u)^{-1} - (1 - p^2u^2/R^2)^{-1/2}\}] \qquad (15)$$
$$I_3 = R \int_0^1 du(1 - u^2)^{-1/2}[(1 - u^2)^{1/2}\{u^2v'(R) - v'(R/u)/u\} / \{G(u)\}^3]$$

where

$$G(u) = [1 - p^2u^2/R^2 - v(R/u)]^{1/2} \qquad (16)$$

The Gauss-Mehler (Chebyshev) quadrature scheme [37] is ideal for integrals like these. The abscissas and weights are simple circular functions and may be evaluated quickly for any desired degree of quadrature. This procedure was used in my integral tables [36] to evaluate the barycentric scattering angles. It has always been used in MARLOWE to evaluate both θ and τ. An equivalent procedure was proposed recently by Mendenhall and Weller [41]: by substituting $u = \cos(\pi z/2)$, the integrals (15) are converted into their forms. The same transformation was also used by Ioup and Thomas [35] and a closely related one by Mason and Schamp [42]. Mendenhall and Weller use Radau (Lobatto) quadrature [37] to evaluate the integrals I_1 and I_3. As is well known, because Radau quadrature specifies the two end points of the integration range, it is somewhat less accurate than a Gaussian quadrature with the same number of abscissas. Either method may be made arbitrarily accurate by increasing the number of abscissas to the required extent and may be applied whenever the integrability condition is satisfied. The Radau abscissas and weights (like those for Gauss-Legendre quadrature) are derived from Legendre polynomials and their evaluation for arbitrary accuracy is complicated. MARLOWE normally uses four Gauss-Mehler points, equivalent to five Radau points in

accuracy, but can use more if desired. For a given number of points, I_1 is significantly more accurate than I_2. MARLOWE does not use I_3.

Both the MARLOWE and the Mendenhall-Weller procedures are more accurate than the approximation proposed by Blanchard et al. [43], who apparently overlooked the integrability of I_1. They are also more accurate than the so-called "magic" formula used in TRIM [27]. Moreover, the quadrature formulae may be applied to different potentials with no additional numerical analysis. This is particularly convenient if potentials are to be used which are not universal, in the sense that their dependence on the atomic numbers of the colliding particles cannot be completely scaled into a single energy parameter and a single space parameter.

4. INTERATOMIC POTENTIAL ENERGY FUNCTIONS

A few remarks must be made about interatomic potential energy functions useful for BCA calculations. The function most widely used in the past is probably the Molière approximation to the Thomas-Fermi potential [44]. The required screening length may be taken from various theoretical analyses or may be regarded as a fitting parameter. The Molière potential is particularly efficient computationally. Recently, however, there have been numerous attempts to base potentials on more fundamental considerations than the Thomas-Fermi model. A more extensive discussion of this topic appears elsewhere [8].

Ziegler et al. (ZBL) [45] used a local density model, with electron distributions from self-consistent Hartree-Fock atomic wavefunctions and free electron corrections to the electron kinetic energy and for exchange and correlation, to evaluate interatomic potential functions. The resulting potentials for many pairs of atoms were then used as the basis for constructing an averaged "universal" potential, represented by

$$V(r) = (Z_1 Z_2 e^2/r) \sum_{j=1}^{4} \alpha_j \exp(-\beta_j r/a_{12}) \qquad (17)$$

where the Z_i are the atomic numbers of the colliding atoms, r is their separation, e is the electron charge,

$$\alpha = \{0.02817, 0.28018, 0.50986, 0.18179\},$$
$$\beta = \{0.2016, 0.4029, 0.9423, 3.2\}, \tag{18}$$

$$a_{12} = (9\pi^2/128)^{1/3}\, a_H / (Z_1^{0.23} + Z_2^{0.23}), \tag{19}$$

and a_H is the Bohr radius. Several comparisons [8,46-50] have found the ZBL potential to be well supported by experimental data as well as by comparisons with *ab initio* potentials.

An alternative to the ZBL potential was developed by Nakagawa and Yamamura [51-53]. Their "average modified Lenz-Jensen" (AMLJ) potential is based on calculations like those of ZBL [45], but using atomic electron distributions with relativistic corrections, as well as confining the atoms to Wigner-Seitz cells representing the densities of the appropriate solids:

$$V(r) = (Z_1 Z_2 e^2/r)\, \exp[-\alpha_1 r + \alpha_2 r^{3/2} - \alpha_3 r^2] \tag{20}$$

where [53]

$$\alpha_1 = (1.706/a_H)\, (Z_1^{0.307} Z + Z_2^{0.307})^{2/3}$$

$$\alpha_2 = (0.916/a_H^{3/2})\, (Z_1^{0.169} + Z_2^{0.169}) \tag{21}$$

$$\alpha_3 = (0.244/a_H^2)\, (Z_1^{0.0418} + Z_2^{0.0418})^{4/3} \quad .$$

It was compared [51] with experimental range data in Si and gives agreement as good as was found for the ZBL potential by O'Connor and Biersack [46]. The AMLJ potential is not universal in the sense that the ZBL potential is, since the α_i have different Z dependences.

The ZBL and AMLJ screening functions are compared in Fig. 2 for Al, Cu, and Au atom pairs. They agree well for small separations, but differences appear at separations approaching the nearest neighbor distances, especially in the lighter elements. It should be noted that the AMLJ potential is more efficient computationally than the ZBL. In preliminary MARLOWE calculations, the execution time was reduced about 20% when the AMLJ potential was used. Thus it may prove a useful alternative to the ZBL potential in BCA models and as a core potential in MD simulations as well.

5. INELASTIC ENERGY LOSSES

Besides losing energy in scattering from the atoms of a target, energetic particles also lose energy by exciting electrons, both those of the medium and those of the particles themselves. See [8] for a more extensive discussion. If such losses depend on the particle kinetic energy and the distance traversed, but are independent of the particular surroundings of a trajectory segment, they are termed "nonlocal" inelastic losses. In MARLOWE, the nonlocal inelastic stopping cross section is taken as

$$S_e(E) = k\,E^{1/2} \tag{22}$$

where the parameter k is derived from experiment, from the well-known LSS theory [54,55], or otherwise. Nonlocal inelastic energy losses and elastic energy losses are uncorrelated.

An alternative formulation of the inelastic stopping problem follows Firsov [56] in making the energy lost inelastically in a collision depend on how closely two atoms approach each other, providing a strong correlation between the elastic and inelastic energy losses. In the formulation used in MARLOWE [57], the energy lost inelastically in a single collision is

$$Q(p,E) = k\,E^{1/2}\,(\gamma^2/2\pi\,a^2)\,\exp[-\gamma R(p,E)/a] \tag{23}$$

where R(p,E) is the apsis in the collision, a is a screening length, and γ is a parameter. In the original Oen-Robinson (OR) model [57], a was the screening length used in the Molière potential and $\gamma = 0.3$. The inelastic stopping cross section is

$$S_e^{OR}(E) = 2\pi \int_0^\infty p\, Q(p,E)\, dp = k\, E^{1/2}\, \sigma(\varepsilon) \tag{24}$$

where ε is the usual reduced energy. Under the conditions of the impulse approximation, the deflection function $\sigma(\varepsilon)$ is unity, but at lower energies it is smaller. Figure 3 shows $\sigma(\varepsilon)$ for the Molière potential for several values of γ. The OR model cuts off the electronic energy losses at low kinetic energy in a plausible manner. The original connection of the OR model with the Molière potential is not essential: any potential can provide a and R(p,E), k can be determined as in the nonlocal model, and γ can be used as a fitting parameter with the nominal task of making the inelastic energy losses follow the electron distributions in the colliding atoms.

It was assumed in writing Eq. (24) that the integration could be extended to infinity. However, in a BCA simulation program, it is necessary to limit impact parameters to values $p < p_c$, where the limit is comparable to the atomic radii in the target, so that part of the local inelastic stopping is missed out. To correct for this, the local inelastic loss is given by Eq. (23) for $p < p_c$, but the part for $p > p_c$ is combined with the nonlocal stopping cross section. The total OR inelastic stopping cross section is then

$$S_e^{OR}(E) = k\, E^{1/2}\, [\sigma(\varepsilon, p_c) + (1 + \gamma\, p_c/a)\, \exp(-\gamma p_c/a)] \tag{25}$$

where the second term is the part regarded as nonlocal.

The local and nonlocal loss models may also be combined by mixing them in any desired proportions, one part establishing k for the local, the other for the nonlocal component. Mixing in equal parts ("equipartition") is a common choice. To the nonlocal part derived in this way must be added that coming from the distant encounters, as described above.

6. SIMULTANEOUS COLLISIONS

Projectiles moving in crystals of high symmetry, such as the common metals, often encounter target atoms in symmetrical groups. Channeled recoils in particular pass through many such groups with symmetries dependent on the crystal structure and the direction of motion. The symmetry of the surroundings is, in fact, responsible for the occurrence of channeling in the first place. Similarly, low-energy recoils are frequently involved in linear collision sequences (LCSs), in which they alternately encounter one or more symmetrical rings of targets and then make central collisions, transferring most of their kinetic energy to a new member of the LCS. One of the features required in a BC program is a consistent method for dealing with such symmetrical encounters between recoils and groups of target atoms, which preserves the symmetry. The occurrence of nearly simultaneous collisions in a BCA model is strongly dependent on the maximum allowed impact parameter, p_c.

As long as p_c is not too large, the particle trajectories can be divided into distinct collisions. In fcc crystals, which constitute a worst case, the radius of an atom with the mean atomic volume is $(3/16\pi)^{1/3} = 0.390796$, in units of the cubic cell edge a_0. The radius of atoms which just touch along <110> directions is $8^{-1/2} = 0.353553$. Thus, truly isolated collisions require $p_c < \sim 0.35$, although in MC codes slightly larger values may be allowed without much concern. At low kinetic energies, larger impact parameters are required for several reasons. First, in both BC and MC codes, an accurate representation of the nuclear stopping cross section is needed, especially when discussing topics like sputtering which are dominated by the behavior of low energy particles. Second, an accurate description of small angle scattering is needed in calculations where surfaces are important, including both sputtering and applications in surface physics. Studies of surface scattering [58,59] show that trajectories may even be qualitatively wrong if interactions with more than the nearest target atoms are excluded. Third, in BC codes, large impact

parameters are needed to obtain reasonable behavior of replacement collision sequences along low index directions of high symmetry crystals. For example, impact parameters up to $(3/8)^{1/2} = 0.612372$, $1/2 = 0.5$, and $6^{-1/2} = 0.408248$ are needed along <110>, <100>, and <111> directions, respectively, of fcc crystals to obtain interactions between perfectly focused sequences and atoms in the rows neighboring them. It is from these interactions that so-called assisted focusing proceeds. Similar values of p_c are also indicated for the proper treatment of channeling. Thus, it is often necessary for a BC program to consider groups of nearly simultaneous encounters.

It is not enough to treat such correlated collisions sequentially. A proper treatment must also preserve the crystal symmetries which often accompany correlated collisions. The preservation of symmetry is also important for channeled projectiles, whether moving in axial or planar channels within a target or in surface channels at its surface. Andersen and Sigmund [60] give an essentially exact treatment of the passage of a projectile through the center of a symmetrical ring of atoms, but their method is not applicable to encounters away from the center of the ring. A more approximate, but more flexible scheme is used in MARLOWE.

The detection and treatment of simultaneous collisions in MARLOWE [29,61] can be explained using the example in Fig. 4. A projectile, moving along the unit vector $\vec{\lambda}_0$ and initially located at P, has two possible collision partners, initially at rest at T_1 and T_2, respectively. These targets are forward along the projectile track by amounts $\zeta_i = \vec{\lambda}_0 \cdot \vec{\Delta x}_i$, where the $\vec{\Delta x}_i$ are the vectors from the projectile to the targets (only that to T_1 is shown). Both distances exceed a minimum required to prevent repetitive encounters with a single atom. The impact parameters, both $< p_c$, are $p_i = |\vec{\lambda}_0 \times \vec{\Delta x}_i|$. The two collisions are evaluated as if each took place alone. The classical turning points (the trajectory asymptote intersections) are forward by the amounts $\hat{\zeta}_i$. Note that the time integral corrections can actually reverse the order of these points, compared with that of the ζ_i. The first turning point along $\vec{\lambda}_0$ is now found. All targets are retained for which $\Delta\hat{\zeta}_{fi} = \hat{\zeta}_i - \hat{\zeta}_f < \Delta\hat{\zeta}_{max}$,

where the subscript f refers to the first turning point. The limit $\Delta\hat{\zeta}_{max}$ is usually taken as 25 pm. The direction and kinetic energy of each target atom are those found for the single isolated encounters and each is placed at the intersection of its laboratory asymptotes, a distance x_2 from its initial position. The direction and momentum of the projectile are determined by applying the conservation of linear momentum to the incident projectile momentum and the set of target momenta. The projectile is placed at the first asymptote intersection along its track. Finally, the conservation of energy is used to scale the momenta of all particles. The algorithm is exact when there is only one target atom, but generally underestimates the energy transferred to multiple targets [7,60].

The algorithm just sketched is illustrated in Fig. 5 by the example of a projectile moving perpendicular to a <011> direction in the fcc metal Cu and passing exactly half way between two nearest-neighbor lattice atoms, T_1 and T_2. The Molière potential was used with the screening length 7.38 pm. In Fig. 5(a), the two collisions are treated sequentially, assuming that the target T_1 is (infinitesimally) closer to the projectile track. In Fig. 5(b), the same event is treated as outlined above. In the former case, the deflection by T_1 makes the projectile pass much closer to T_2 than it does in the latter. The projectile loses more energy because of this and is also deflected away from the original direction of motion. The simultaneous treatment preserves the original direction of motion, but underestimates the energy lost by the projectile. (Note: the similar example shown in Fig. 5 of reference [25] and reproduced in references [5,62] is based on an earlier and less satisfactory treatment of simultaneous collisions.)

The MARLOWE algorithm preserves the crystal symmetries associated with cascade development, including both energetic channeled projectiles and low energy LCSs. Because energy losses to neighboring rows are underestimated, the lengths of LCSs are overestimated. This can be compensated in part by including a small binding energy for the second and subsequent members of such sequences.

7. SCHEDULING ALGORITHMS IN BCA MODELS

Even if the time is not evaluated explicitly, as is common in BCA codes, the collisions of any one particle are correctly ordered in time, but a scheduling algorithm is necessary to organize the collisions of one projectile with respect to those of another. The earliest BCA codes used rather arbitrary scheduling rules, designed to minimize computing time or storage requirements, and little attempt was made to simulate the temporal development of cascades correctly. This is still true of some codes today.

The rule used in MARLOWE from the beginning was to follow at each collision the fastest particle currently in motion in the cascade. It is implemented in a nearly exact manner without sorting or searching large tables. The basis of the algorithm is the well-known asymptotic recoil spectrum proportional to E^{-2}. A table address is computed as if it were a histogram channel number:

$$j = m\,S\,/\,m_1\,E$$

where m is the mass and E the kinetic energy of the projectile in question, m_1 is the mass of a reference particle, and S is a scale factor controlled by the cut-off energy and the length of the projectile priority table. A pointer identifying the particle is stored at the indicated place in the table. Fast particles are stored near the start of the table, slow ones near the end. The width of a position in the table is proportional to E^2, so that much more space is available for the many slow particles than for the few fast ones. Nevertheless, conflicts occur between particles for positions in the table, which are resolved by moving the later particles to the first available position towards the middle of the table. Conflicts are reduced by making the table twice as long as the minimum necessary, but their occurrence and resolution make the algorithm approximate. After each collision, pointers to the emerging particles are stored in the priority table using the algorithm outlined. For the next collision, the particle nearest the start of the table is selected. Cascade development continues as long as particles remain in the table.

The "fastest first" algorithm causes MARLOWE to defer the processing of a slow particle until none remains with a greater speed. Thus, the number of atoms in motion tends to increase steadily until all energies are fairly low and many particles then stop almost together. The fast particles tend to run away from the slow ones and to move in undamaged regions of the target. This minimizes the opportunity for moving particles to interact with stopped ones.

An alternative algorithm that could be implemented in the same way would process the slowest current projectile first (Smith and Webb [63] mention this scheduling rule). This option is not available in MARLOWE, since it seems very hard to justify, although it would provide many stopped cascade particles early in cascade development and would maximize their influence on the fast particles.

A better procedure than "fastest first" is to schedule the collisions in their proper order in time [64]. Two time intervals control the scheduling. First, the value of Δt establishes the granularity of the MARLOWE time scale. Any collision occurring within the current time interval is processed in the usual way. If a collision is found to occur after the current interval, a pointer identifying the projectile is put in a table referring to the predicted collision time interval. To avoid problems which can occur, particles are never assigned to a time interval more than Δt^* after the present. $\Delta t^* \geq \Delta t > 0$ is required. Projectiles are re-examined when the time interval arrives to which they were assigned. If $\Delta t^* = \Delta t$, all moving recoils are examined in every time interval and the collisions in a cascade are in precise time order, except for irregularities smaller then Δt, but the code runs slowly because encounters are re-examined so often. On the other hand, if $\Delta t^* >> \Delta t$, particles are re-examined only when the predicted time interval arrives. The code runs faster, but errors in the time ordering are more serious. These occur mainly because, after the prediction is made, but before the predicted time arrives, other events supervene such as the displacement of predicted target atoms by other projectiles or the stopping of projectiles that were still moving when the prediction was made.

Management of the time-ordered priority table is more complicated than that of the velocity-ordered one. The space allowed for particles assigned to each time interval is managed dynamically through a two-level pointer system, one level controlling the space assigned for a time interval, the other pointing to the projectiles in each interval. After the end of an interval, the space it used is released and may be reused later. As each time interval arrives, the particles predicted to collide during it are processed, in either 'first in, first out' or 'last in, first out' order, as desired. The differences should be insignificant.

Studies of time-ordered cascades [64,65] show that slowly moving particles are present in cascades from very early times and that their numbers increase steadily throughout cascade development. As a result, there are far more encounters between energetic recoils and previously stopped cascade particles than are found in "fastest first" cascades, particularly in high-energy cascades in heavy elements like gold.

8. SEARCHING FOR DEFECTS

An important task for a code of the BC type is to conserve atoms: this means that no lattice site may emit more than one displaced atom. Closely related tasks are the pairing of displaced atoms with vacant lattice sites and the location of stopped cascade atoms for assessment as possible collision partners for moving recoils. These tasks are all carried out in MARLOWE by maintaining so-called 'hashed' tables of pointers to lattice sites. For any lattice site, a 'hash' address in a table of length L is calculated as:

$$m = \{[c\, x_1] \bmod b\} + b\, \{[c\, x_2] \bmod b\} + b^2\, \{[c\, x_3] \bmod b\} \qquad (26)$$

where the x_i are the coordinates of the site, [ ] indicates 'the integral part of,' mod is an abbreviation for modulo, c is a multiplier taken as 4 in MARLOWE, and $b = [L^{1/3}]$. The table is initially empty (each location contains 0). When a site is added to the table, a pointer to the site is stored in the indicated place, if it is available. If not, m is incremented until a place is found. For $m > L$, $m - L$ replaces m; that is, the table is cyclic. The basic idea

embodied in Eq. (26) is closely similar to that underlying the "box search" algorithm used in the famous GRAPE program [66].

To determine if a site is in the table, Eq. (26) is used to construct the address where it would be expected. If the location is empty, the site is not there. If it is occupied, the coordinates of the indicated site are checked against those of the test site. If there is no match, m is incremented and the procedure is repeated until either a zero or a match is found. The value of L is large enough that the table is never more than half full. Little actual searching is necessary to determine whether a site is in the table.

MARLOWE uses two implementations of this algorithm. First, a table of vacant lattice sites is maintained. The pointers in this table identify the sites, each appearing once. This table is used to eliminate vacant sites that are proposed as the collision partners of moving recoils. It is also used at the end of cascade development in pairing displaced atoms with vacant sites. The second use of the algorithm is in maintaining a table of stopped cascade atoms eligible to become targets in collisions. In this case, the sites are those nearest to each atom. These sites may appear more than once in the table, since each may be the site nearest to several atoms. The pointers identify the eligible stopped cascade atoms.

The tables built and maintained by the algorithm described above constitute a sort of associative memory, allowing sites to be identified precisely and quickly. The time to recover a site from the table is essentially independent of the number of entries in it and no sorting of the table entries is ever required.

9. CONCLUSION

Several aspects of the binary collision approximation have been discussed, as they are implemented in the current version of MARLOWE. To complete the discussion, it is appropriate to mention some comparisons that have been made between BCA codes and inherently more accurate MD models.

Schiffgens et al. [67] made a number of studies of LCSs in Cu, using the codes COMENT [68] and ADDES [69]. The former is a full MD program; the latter is a so-called quasistable dynamical model [7], using an energy criterion to control the number of atoms included in the integrations. The comparisons were part of the basis for choosing parameters for ADDES simulations. As an extension of this work, the same events have been simulated in MARLOWE, using the same potential and one of the screening lengths used in the MD codes. and varying several MARLOWE parameters. Some results are displayed in Table 1. Two sets of MARLOWE simulations are shown. In the first, there were no binding energies in the model. In the second, target atoms were bound to their lattice sites by an energy E_b when displacements occurred, that is, when both the projectile and the target atom emerge from a collision; when the projectile replaced the target on the lattice site, however, the binding energy was reduced to $E_b' = 0.1\ E_b$. The cohesive energy, 3.5 eV, was used for E_b. In each case, the table shows ΔE_0, the difference between the initial kinetic energy of the primary particle and that of the next atom in the sequence. In MD models, this loss is always the greatest in any LCS and comes about physically by storing energy in the first ring of atoms around the track. In later steps, the energy loss is much less, since this stored energy is passed along from ring to ring as the LCS progresses. The second MARLOWE model reproduces the COMENT energy losses rather well. The table also shows N, the number of replacements occurring in each sequence. The <011> sequences in MARLOWE are a little shorter than those in COMENT: this could likely be remedied by slight adjustments of the binding energies. The <001> and <111> sequences, however, are and would remain substantially longer in MARLOWE than in COMENT. This behavior is consistent with the errors expected in the MARLOWE treatment of simultaneous collisions. These errors are least when the rings of neighbors are largest, as in <011> sequences in fcc metals, and are largest when the rings are smallest as in <111> sequences in the same materials. See reference [7] for more details.

The round-robin collaboration on ejection probability in sputtering [26] also compared BCA programs with MD models. It is notable that results obtained with BC models were quite similar to those with MD models in many respects, although the problem investigated is not a very stringent test. The original report should be consulted for the details.

Further detailed comparisons of BC models with MD models could be made. For example, in addition to the numbers of replacements in an LCS, one could examine the detailed distribution of the atoms at various times after the passage of the main disturbance. The 50 eV <011> LCS in Table 1 is notably different from the others in the MARLOWE simulation, in that not all of the events along the sequence are simple replacements, but involve displacement of the sequence atoms. These later lose energy to their neighbors and come to rest close to their original sites. Many other comparisons can be imagined and would give interesting information about the relationships of various kinds of codes. These might be useful for improving the realism of the BC models.

ACKNOWLEDGMENTS

This research was sponsored by the Division of Materials Sciences, U.S. Department of Energy under Contract No. DE-AC05-84OR21400 with Martin Marietta Energy Systems, Inc.

10. REFERENCES

[1] B. J. Alder and T. E. Wainwright, *J. Chem. Phys.* **27**, 1208 (1957).

[2] M. M. Bredov, I. G. Lang, and N. M. Okuneva, *Zh. Tekh. Fiz.* **28** (1958) Engl. transl.: *Sov. Phys.-Tech. Phys.* **3**, 228 (1958)].

[3] D. T. Goldman, D. E. Harrison, Jr., and R. R. Coveyou, U. S. Atomic Energy Commission Report ORNL-2729 (1959).

[4] J. B. Gibson, A. N. Goland, M. Milgram, and G. H. Vineyard, *Phys. Rev.* **120**, 1229 (1960). See also *J. Appl. Phys.* **30**, 1322 (1959) and cover.

[5] J. R. Beeler, Jr., and D. G. Besco, *Radiation Damage in Solids*, Vol. I (I. A. E. A., Vienna, 1962), p. 43.

[6] M. T. Robinson, D. K. Holmes, and O. S. Oen, *Le Bombardement Ionique* (C. N. R. S., Paris, 1962), p. 105.

[7] M. T. Robinson in *Sputtering by Particle Bombardment I*, edited by R. Behrisch (Springer, Berlin, etc., 1981), pp. 73-144.

[8] M. T. Robinson, *K. Dan. Vidensk. Selsk. Mat. Fys. Medd.* (1992) to be published.

[9] W. Eckstein, *Computer Simulation of Ion-Solid Interactions* (Springer, New York, etc. 1991).

[10] J. R. Beeler, Jr., *Radiation Effects Computer Experiments* (North-Holland, Amsterdam, etc., 1983).

[11] N. Bohr, *K. Dan. Vidensk. Selsk. Mat. Fys. Medd.* **18**, no. 8 (1948).

[12] E. H. Kennard, *Kinetic Theory of Gases* (McGraw-Hill, New York, 1938), especially pp. 97-134.

[13] G. H. Wannier, *Statistical Physics* (Wiley, New York, 1966), especially pp. 385-468.

[14] J. R. Beeler, Jr., and D. G. Besco, *J. Phys. Soc. Japan* **18**, Suppl. III, 159 (1963).

[15] J. R. Beeler, Jr., and D. G. Besco, *J. Appl. Phys.* **34**, 2873 (1963).

[16] J. A. Brinkman, *J. Appl. Phys.* **25**, 961 (1954).

[17] G. Leibfried and O. S. Oen, *J. Appl. Phys.* **33**, 2257 (1962).

[18] C. Lehmann and G. Leibfried, *Z. Physik* **172**, 465 (1963).

[19] C. Lehmann and M. T. Robinson, *Phys. Rev.* **134**, A37 (1964).

[20] D. K. Holmes and G. Leibfried, *J. Appl. Phys.* **31**, 1046 (1960).

[21] O. S. Oen, D. K. Holmes, and M. T. Robinson, *J. Appl. Phys.* **34**, 302 (1963).

[22] O. S. Oen and M. T. Robinson, *J. Appl. Phys.* **35**, 2515 (1964).

[23] M. T. Robinson and O. S. Oen, *Appl. Phys. Lett.* **2**, 30 (1963).

[24] M. T. Robinson and O. S. Oen, *Phys. Rev.* **132**, 2385 (1963).

[25] M. T. Robinson and I. M. Torrens, *Phys. Rev. B* **9**, 5008 (1974).

[26] P. Sigmund, M. T. Robinson, M. I. Baskes, M. Hautala, F. Z. Cui, W. Eckstein, Y. Yamamura, S. Hosaka, T. Ishitani, V. I. Sulga, D. E. Harrison, Jr., I. R. Chakarov, D. S. Karpuzov, E. Kawatoh, R. Shimizu, S. Valkealahti, R. M. Nieminen, G. Betz, W. Husinsky, M. H. Shapiro, M. Vicanek, and H. Urbassek, *Nucl. Instrum. Methods B* **36**, 110 (1989).

[27] J. P. Biersack and L. G. Haggmark, *Nucl. Instrum. Methods* **174**, 257 (1980).

[28] W. Takeuchi and Y. Yamamura, *Radiat. Eff.* **71**, 51 (1983).

[29] M. T. Robinson, *Phys. Rev. B* **40**, 10717 (1989).

[30] *MARLOWE* (Version 13) is available from the Radiation Shielding Information Center, Oak Ridge National Laboratory, Post Office Box 2008, Oak Ridge, Tennessee 37831-6362, U. S. A.

[31] Y. Yamamura, *Nucl. Instrum. Methods B* **33**, 493 (1988).

[32] H. Goldstein, *Classical Mechanics*, Second Edition (Addison-Wesley, Reading, Massachusetts, 1980), pp. 105-119.

[33] J. B. Marion, *Classical Dynamics of Particles and Systems* (Academic Press, New York, 1970), pp. 243-312.

[34] S. H. Overbury, F. W. Meyer, and M. T. Robinson, *Nucl. Instrum. Methods B* **67**, 126 (1992).

[35] G. E. Ioup and B. S. Thomas, *J. Chem. Phys.* **50**, 5009 (1969).

[36] M. T. Robinson, *Tables of Classical Scattering Integrals*, U. S. Atomic Energy Commission Report ORNL-4556 (1970).

[37] Z. Kopal, *Numerical Analysis* (Wiley, New York, 1961), Chapter VII.

[38] F. J. Smith, *Physica* **30**, 497 (1964).

[39] F. J. Smith and R. J. Munn, *J. Chem. Phys.* **41**, 3560 (1964).

[40] M. Kennedy and F. J. Smith, *Mol. Phys.* **13**, 443 (1967).

[41] M. H. Mendenhall and R. A. Weller, *Nucl. Instrum. Methods B* **58**, 11 (1991).

[42] E. A. Mason and H. W. Schamp, Jr., *Ann. Phys.* (N. Y.) **4**, 233 (1958).

[43] J. P. Blanchard, N. M. Ghoniem, and S. P. Chou, *J. Appl. Phys.* **61**, 3120 (1987).

[44] G. Molière, *Z. Naturforsch.* **2a**, 133 (1947).

[45] J. F. Ziegler, J. P. Biersack, and U. Littmark, *Stopping Powers and Ranges of Ions in Matter* (Pergamon, New York, etc., 1985), pp. 25ff.

[46] D. J. O'Connor and J. P. Biersack, *Radiat. Eff.* **62**, 14 (1986).

[47] K. Broomfield, R. A. Stansfield, and D. C. Clary, *Surface Sci.* **202**, 320 (1988).

[48] R. A. Stansfield, K. Broomfield, and D. C. Clary, *Phys. Rev. B* **39**, 7680 (1989).

[49] K. Broomfield, R. A. Stansfield, and D. C. Clary, *Surface Sci.* **227**, 369 (1990).

[50] J. Keinonen, A. Kuronen, P. Tikkanen, H. G. Boerner, J. Jolie, S. Ulbig, E. G. Kessler, R. M. Niemenen, M. J. Puska, and A. P. Seitsonen, *Phys. Rev. Lett.* **67**, 3692 (1991).

[51] S. T. Nakagawa and Y. Yamamura, *Radiat. Eff.* **105**, 239 (1988).

[52] S. T. Nakagawa, *Radiat. Eff.* **112**, 1 (1990).

[53] S. T. Nakagawa, *Radiat. Eff.* **116**, 21 (1991). This paper uses atomic units and omits the Bohr radius from several formulas.

[54] J. Lindhard and M. Scharff, *Phys. Rev.* **124**, 128 (1961).

[55] J. Lindhard, V. Nielsen, and M. Scharff, *K. Dan. Vidensk. Selsk. Mat. Fys. Medd.* **36**, no. 10 (1968).

[56] O. B. Firsov, *Zh. Eksp. Teor. Fiz.* **36** (1959) 1517 [Engl. transl.: *Sov. Phys.-JETP* **36**, 1076 (1959)]

[57] O. S. Oen and M. T. Robinson, *Nucl. Instrum. Methods* **132**, 647 (1976).

[58] D. S. Karpuzov and V. E. Yurasova, *Phys. Stat. Solidi* **47**, 41 (1971).

[59] C.-C. Chang, N. Winograd, and B. J. Garrison, *Surface Sci.* **202**, 309 (1988).

[60] H. H. Andersen and P. Sigmund, *K. Dan. Vidensk. Selsk. Mat. Fys. Medd.* **34**, no. 15 (1966).

[61] M. Hou and M. T. Robinson, *Nucl. Instrum. Methods* **132**, 641 (1976).

[62] V. E. Yurasova and V. A. Eltekov, *Vacuum* **32**, 399 (1982).

[63] R. Smith and R. Webb, *Nucl. Intrum. Methods B* **67**, 373 (1992).

[64] M. T. Robinson, *Nucl. Instrum. Methods B* **48**, 408 (1990).

[65] M. T. Robinson, *Nucl. Instrum. Methods B* **67**, 396 (1992).

[66] A. Larsen, *GRAPE, A Computer Program for Classical Many-Body Problems in Radiation Damage*, U. S. Atomic Energy Commission Report BNL-7979 (1964), pp. 8-11. See also ref. [10], pp. 661ff.

[67] J. O. Schiffgens, D. M. Schwartz, R. G. Ariyasu, and S. E. Cascadden, *Radiat. Eff.* **39**, 221 (1978).

[68] J. O. Schiffgens and R. D. Borquin, *J. Nucl. Mater.* **69/70**, 790 (1978).

[69] D. M. Schwartz, J. O. Schiffgens, D. G. Doran, G. R. Odette, and R. G. Ariyasu, *Computer Simulation for Materials Applications*, edited by R. J. Arsenault, J. R. Beeler, Jr., and J. A. Simmons, *Nucl. Metall.* **20**, 75 (1976).

Table 1. Comparisons of Replacement Sequences in Cu, as Evaluated by the Codes COMENT and MARLOWE.

Molière Potential, a_{12} = 7.38 pm.

Nominal Direction	Deviation ϑ	(deg) ϕ	Initial Energy (eV)	COMENT[a] ΔE_0	COMENT[a] N	MARLOWE[b] ΔE_0	MARLOWE[b] N	MARLOWE[c] ΔE_0	MARLOWE[c] N
<011>	1	1	25	3.63	~34[d]	0.15	76	4.01	22
	3	3	38	5.08	13[e]	0.60	14	4.36	16
	5	5	50	8.58	7	2.70	6	6.25	4
<001>	1	1	40	6.09	6	1.67	15	5.60	12
	2	4	30	6.61	4	1.01	10	5.95	8
<111>	1.76	1	150	24.27	5	12.63	9	26.63	8

(a) COMENT results from Schiffgens et al. [67] and J. O. Schiffgens, private communication (1980).

(b) MARLOWE (Version 13) with $E_b = E_b' = 0$.

(c) MARLOWE (Version 13) with $E_b = 3.5$ eV and $E_b' = 0.35$ eV.

(d) Estimated. This event was not fully contained within the COMENT numerical crystallite [67].

(e) Uncertain. The atoms move very slowly for a long time, making identification of replacements difficult.

FIGURE TITLES

Fig. 1. The trajectories of a projectile and an initially stationary target atom interacting according to a conservative central repulsive force. The positions of the particles and of their barycenter are shown at the apsis of the encounter.

Fig. 2. A comparison of the AMLJ [51,53] and the ZBL [45] screening functions for Al, Cu, and Au. The nearest neighbor distances in the crystals are 0.286, 0.256, and 0.288 nm, respectively.

Fig. 3. The deflection factor in the OR inelastic stopping cross section model [57], evaluated for the Molière potential. The original OR work used $\gamma = 0.3$.

Fig. 4. The treatment of nearly simultaneous collisions in MARLOWE [29]. See the text for an explanation.

Fig. 5. Comparisons of the sequential and simultaneous treatments of a three particle encounter. The example correspond to the motion of a Cu atom perpendicular to a <011> direction in a Cu crystal.

ORNL-DWG 63-2718R4

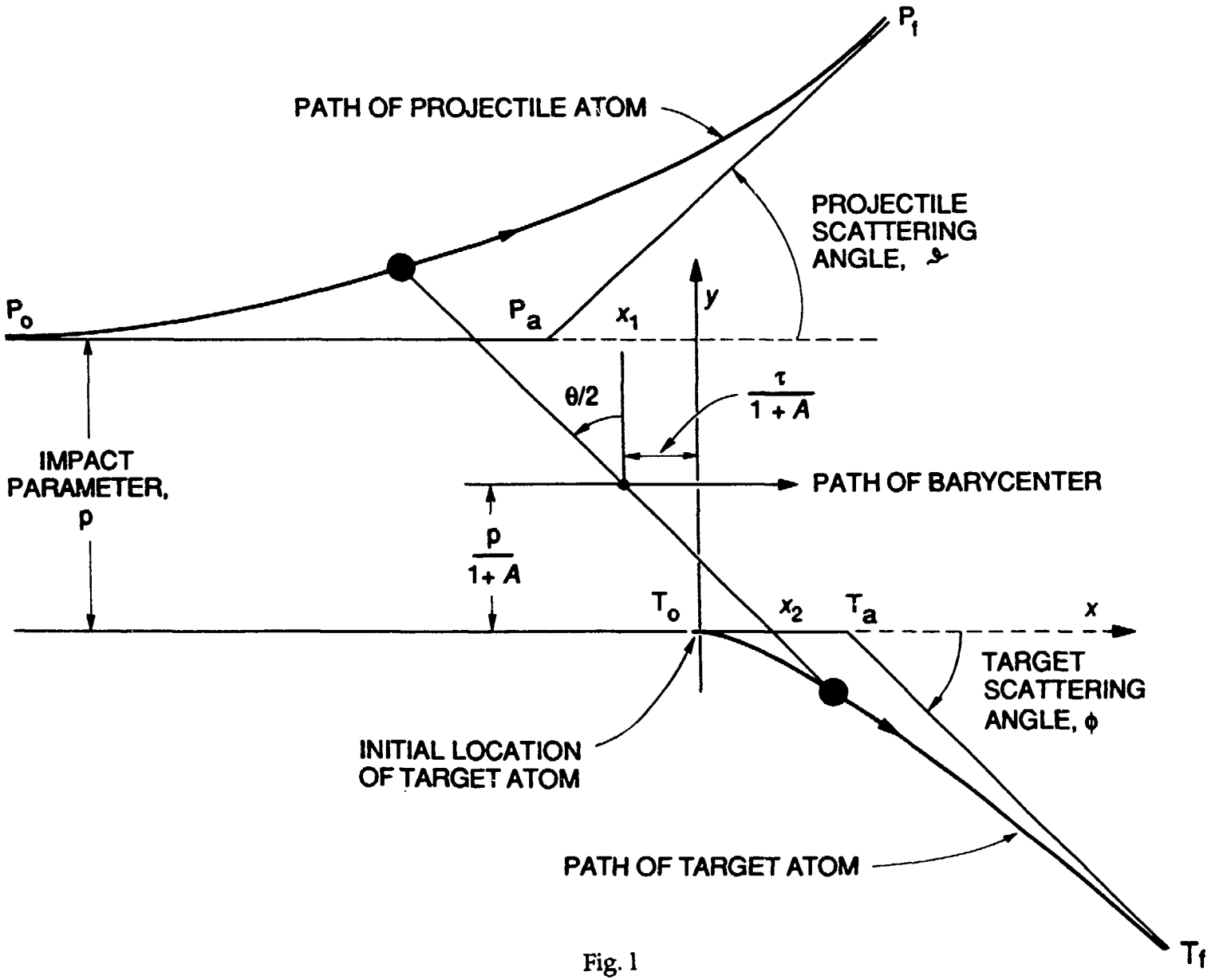

Fig. 1

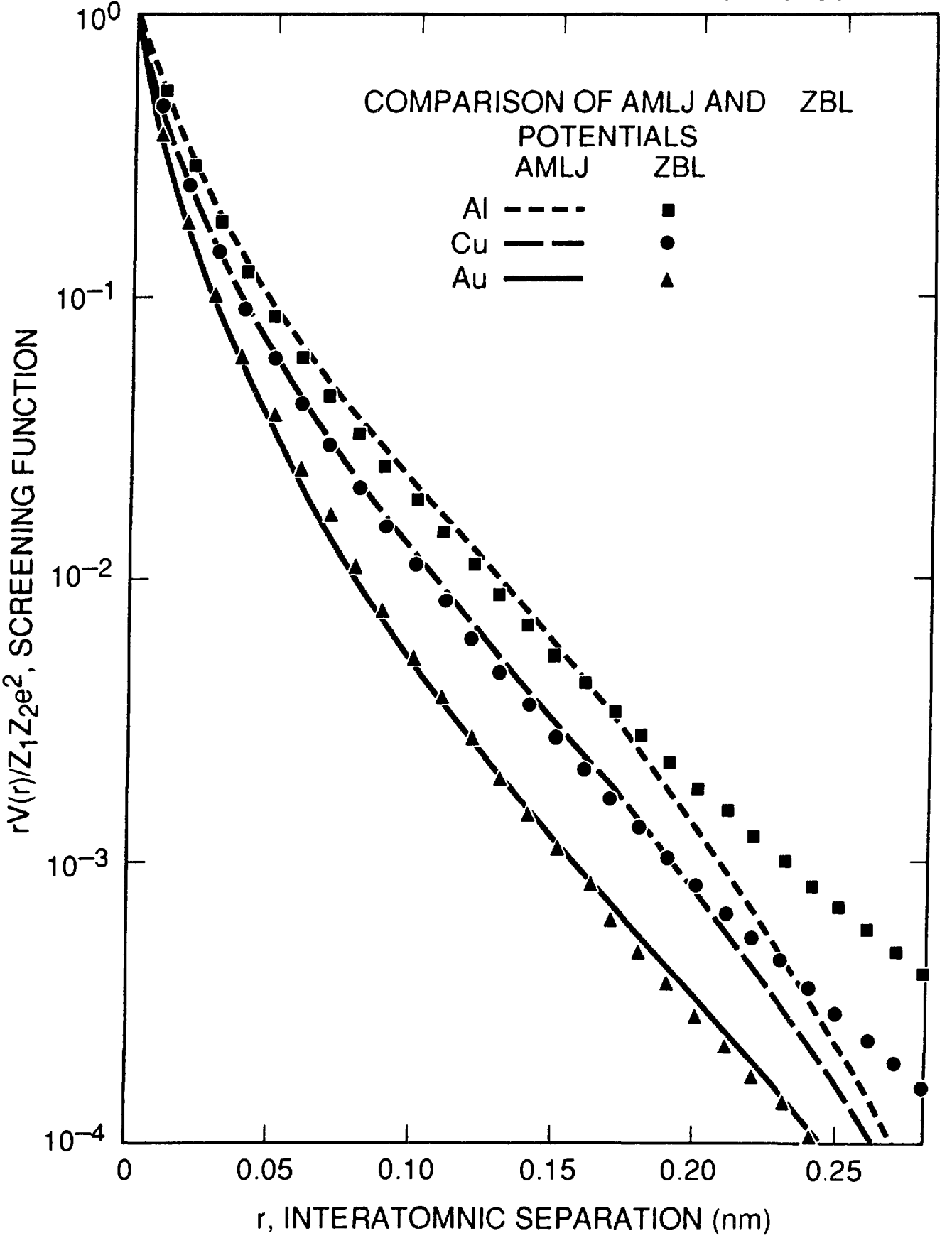
COMPARISON OF AMLJ AND ZBL POTENTIALS
AMLJ ZBL
Al
Cu
Au
10^0
10^{-1}
10^{-2}
10^{-3}
10^{-4}
$rV(r)/Z_1Z_2e^2$, SCREENING FUNCTION
0
0.05
0.10
0.15
0.20
0.25
r, INTERATOMNIC SEPARATION (nm)

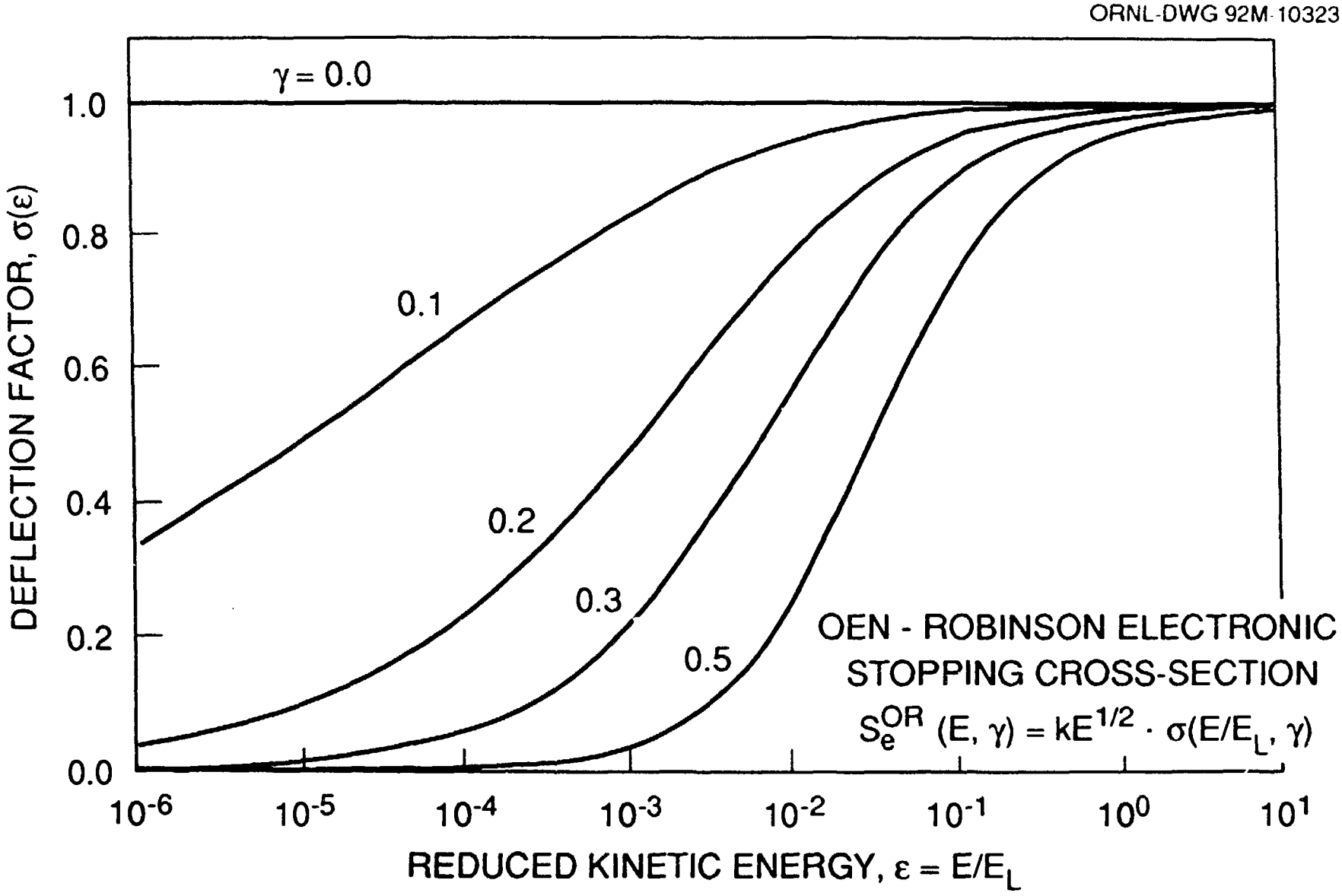
ORNL-DWG 92M-10323
γ = 0.0
1.0
0.8
0.6
0.4
0.2
0.0
DEFLECTION FACTOR, σ(ε)
0.1
0.2
0.3
0.5
OEN - ROBINSON ELECTRONIC
STOPPING CROSS-SECTION
$S_e^{OR}(E, \gamma) = kE^{1/2} \cdot \sigma(E/E_L, \gamma)$
10^{-6}
10^{-5}
10^{-4}
10^{-3}
10^{-2}
10^{-1}
10^{0}
10^{1}
REDUCED KINETIC ENERGY, $\varepsilon = E/E_L$

Fig. 3

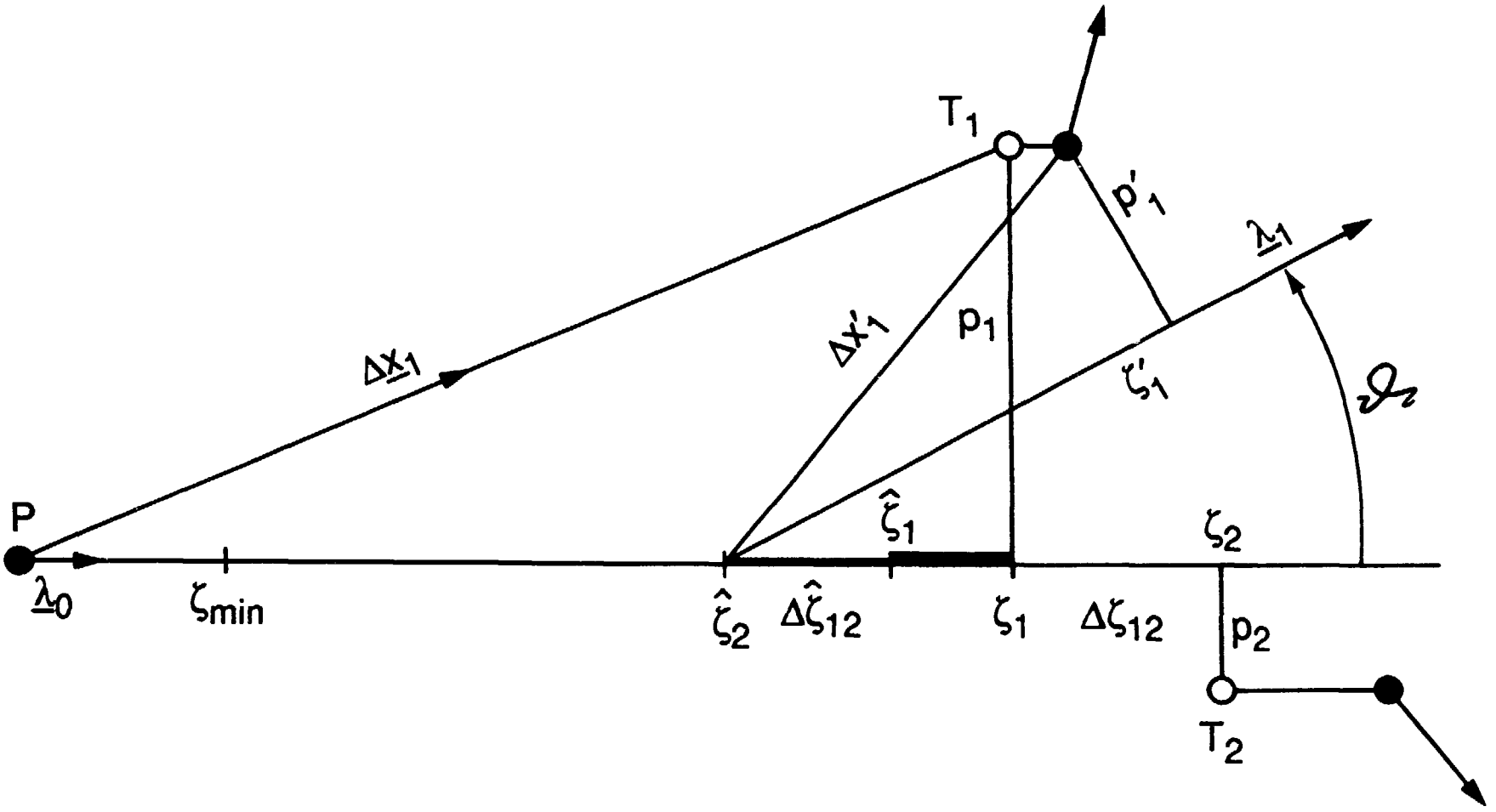

Fig. 4

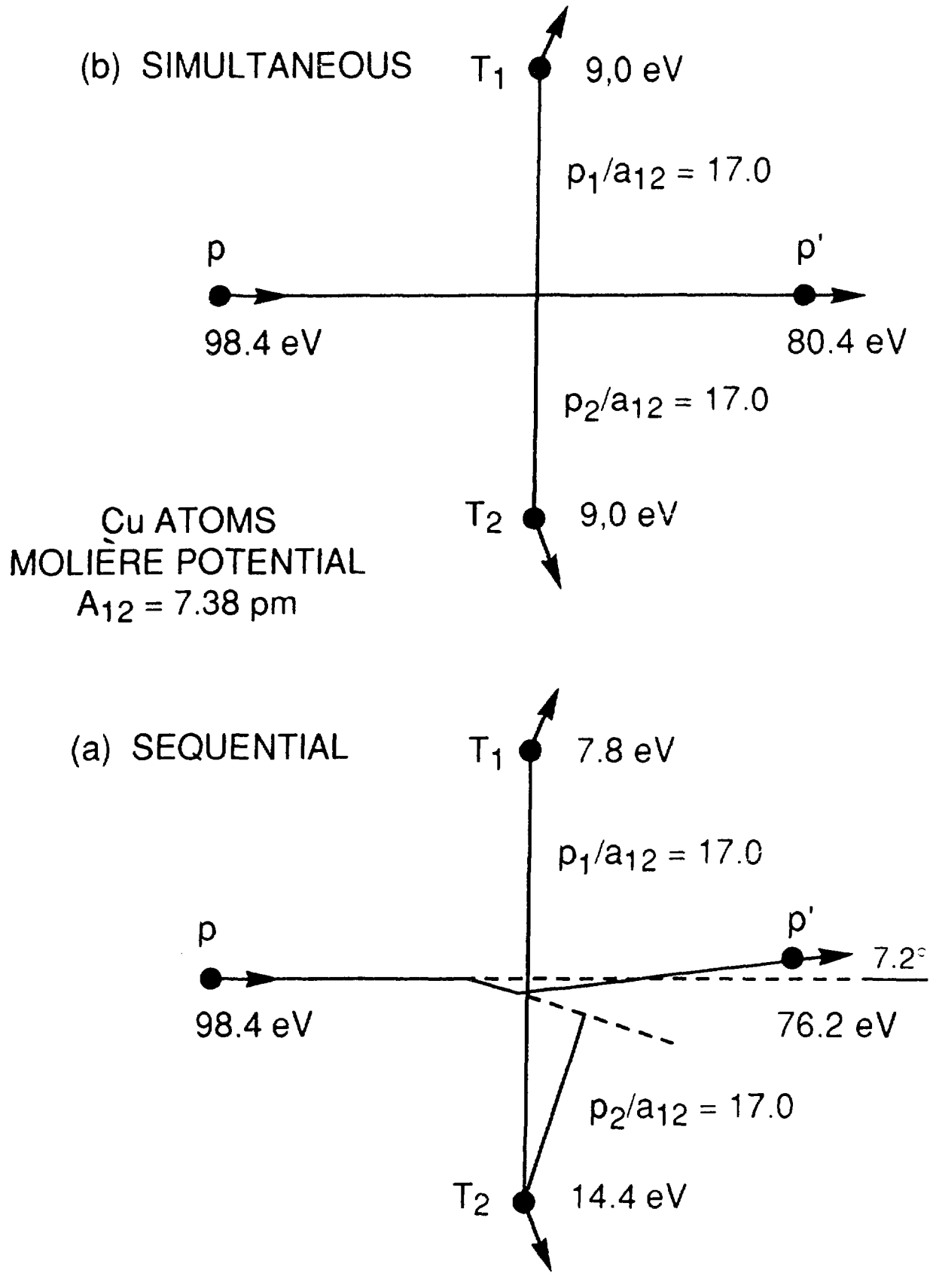
(b) SIMULTANEOUS
T1
9,0 eV
p1/a12 = 17.0
p
p'
98.4 eV
80.4 eV
p2/a12 = 17.0
T2
9,0 eV
Cu ATOMS
MOLIÈRE POTENTIAL
A12 = 7.38 pm
(a) SEQUENTIAL
T1
7.8 eV
p1/a12 = 17.0
p
p'
7.2°
98.4 eV
76.2 eV
p2/a12 = 17.0
T2
14.4 eV

Fig. 5